Acta Crystallographica Section F
Structural Biology and Crystallization Communications
ISSN 1744-3091

Structure of myotoxin II, a catalytically inactive Lys49 phospholipase A_2 homologue from *Atropoides nummifer* venom

Mário T. Murakami,[a] Cristiane C. Melo,[a] Yamileth Angulo,[b,c] Bruno Lomonte[b]* and Raghuvir K. Arni[a,d]*

[a]Department of Physics, IBILCE/UNESP, São José do Rio Preto-SP, Brazil, [b]Instituto Clodomiro Picado, Facultad de Microbiologia, San José, Costa Rica, [c]Departamento de Bioquímica, Escuela de Medicina, Universidad de Costa Rica, San José, Costa Rica, and [d]Center for Applied Toxinology, Butantan Institute, São Paulo-SP, Brazil

Correspondence e-mail: blomonte@cariari.ucr.ac.cr, arni@ibilce.unesp.br

Received 10 February 2006
Accepted 23 March 2006

PDB Reference: myotoxin II, 2aoz, r2aozsf.

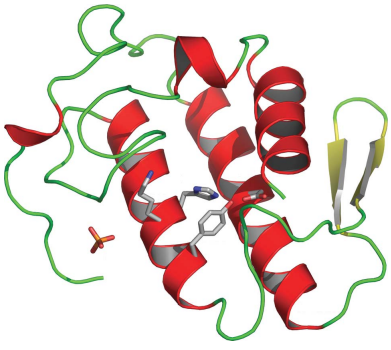

Lys49 snake-venom phospholipase A_2 (PLA_2) homologues are highly myotoxic proteins which, although lacking catalytic activity, possess the ability to disrupt biological membranes, inducing significant muscle-tissue loss and permanent disability in severely envenomed patients. Since the structural basis for their toxic activity is still only partially understood, the structure of myotoxin II, a monomeric Lys49 PLA_2 homologue from *Atropoides nummifer*, has been determined at 2.08 Å resolution and the anion-binding site has been characterized.

1. Introduction

Skeletal muscle necrosis is a frequent consequence of envenomation by snakes of the family Crotalidae and may lead to significant tissue loss and permanent disability (Mebs & Ownby, 1990; Nishioka & Silveira, 1992). The venoms of these snakes contain a number of basic phospholipases A_2 (PLA_2s; EC 3.1.1.4) that play prominent roles in the pathogenesis of myonecrosis (Gutiérrez & Lomonte, 1995). These myotoxic proteins are classified as belonging to the group IIA PLA_2s on the basis of their primary structure and disulfide-bonding pattern (Six & Dennis, 2000). A subgroup of catalytically inactive variants or PLA_2 homologues was initially characterized from the venom of the North American water mocassin *Agkistrodon piscivorus piscivorus*, in which the conserved Asp at position 49 is replaced by Lys (Maraganore *et al.*, 1984; Scott *et al.*, 1992; Arni & Ward, 1996). Homologous 'Lys49 PLA_2 myotoxins' have now been encountered in the venoms of a wide variety of crotalid species (reviewed by Lomonte *et al.*, 2003) and have attracted attention since they serve as models for the investigation of the structural basis of the catalytically independent mechanisms of membrane damage. Recently, it has been demonstrated that these basic Lys49 PLA_2s bind to the extracellular domain of the vascular endothelial growth factor ($VEGF_{165}$) receptor with a sub-nanomolar affinity (Yamazaki *et al.*, 2005).

Two Lys49 PLA_2 homologues have previously been isolated from the venom of *Atropoides nummifer*, a crotalid snake distributed along the Central American isthmus (Taylor *et al.*, 1974; Solórzano, 1989). *A. nummifer* myotoxin I (Gutiérrez *et al.*, 1986) has been crystallized and its structure has been reported at 2.4 Å resolution (Arni & Gutiérrez, 1993; de Azevedo *et al.*, 1999); however, since its amino-acid sequence has not been determined, accurate structural data is as yet unavailable. On the other hand, *A. nummifer* myotoxin II (Anum-II) has been well characterized in terms of its biological activities (Angulo *et al.*, 2000) and its complete amino-acid sequence has been determined (SwissProt code P82950; Angulo *et al.*, 2002). This protein has recently been crystallized (Watanabe *et al.*, 2004) and the present report presents a detailed analysis of its three-dimensional structure, which has been determined at 2.08 Å resolution.

2. Materials and methods

2.1. Purification, crystallization and data collection

A. nummifer venom was obtained from more than 15 specimens collected in Costa Rica. Anum-II was purified by cation-exchange

Table 1
Data-collection and refinement statistics of the Anum-II crystal structure.

Values in parentheses are for the highest resolution shell.

Data collection	
Space group	$P4_32_12$
Unit-cell parameters (Å)	$a = b = 68.94$, $c = 64.07$
V_M (Å^3 Da^{-1})	2.66
Solvent content (%)	53.40
Resolution range (Å)	30.36–2.08 (2.19–2.08)
No. of unique reflections	9671
Completeness (%)	99.3 (94.1)
R_{merge}† (%)	8.9 (48.1)
$I/\sigma(I)$	6.7 (2.3)
Refinement	
R factor‡ (%)	21.9
R_{free}§ (%)	27.0
B values¶ (Å^2)	
Overall	30.48
Main chain	28.64
Side chain	29.2
R.m.s.d. in bond length (Å)	0.021
R.m.s.d. in bond angles (°)	1.868

† $R_{merge} = 100 \times \sum[\sum |I(h) - \langle I(h)\rangle|]/\sum I(h)$, where $I(h)$ is the observed intensity and $\langle I(h)\rangle$ is the mean intensity of reflection h over all measurements of $I(h)$. ‡ R factor = $100 \times \sum(|F_o - F_c|)/\sum(F_o)$, the sums being taken over all reflections with $F/\sigma(F) > 2$ cutoff. § R_{free} = R factor for 5% of the data which were not included during crystallographic refinement. ¶ B values are average B values for all non-H atoms.

chromatography on carboxymethyl-Sephadex C-25 (Pharmacia) (Angulo *et al.*, 2000) and reverse-phase high-performance liquid chromatography (RP-HPLC) on a C4 column (Vydac) which was eluted at a flow rate of 1.0 ml min^{-1} with a gradient ranging from 0 to 60% acetonitrile in 0.1% trifluoroacetic acid, using a Waters 600E instrument (Watanabe *et al.*, 2004).

The Anum-II sample was dissolved in water at a concentration of 10 mg ml^{-1}. Crystallization experiments were carried out by the hanging-drop vapour-diffusion method. Single crystals were obtained when a 2 µl protein droplet was mixed with an equal volume of a solution consisting of 0.1 *M* sodium acetate pH 4.6, 20% PEG 3350 and 0.2 *M* ammonium sulfate and subsequently equilibrated over 1 ml of the latter solution at 291 K (Watanabe *et al.*, 2004). Crystals of Anum-II were flash-cooled in crystallization solution to which 15%(*v*/*v*) glycerol had been added. Diffraction data were collected from a single cryoprotected Anum-II crystal utilizing a wavelength of 1.427 Å (at 100 K) at a synchrotron-radiation source (Laboratório Nacional de Luz Síncrotron, Campinas, Brazil). Intensity data were reduced and processed at 2.08 Å using the program *MOSFLM* (Leslie, 1992). The crystals of Anum-II belong to space group $P4_32_12$ and are compatible with the presence of one protein molecule in the asymmetric unit. The data-collection and processing statistics are summarized in Table 1.

2.2. Structure determination and crystallographic refinement

The crystal structure of Anum-II was determined by molecular replacement using the program *MOLREP* (Vagin & Teplyakov, 1997). The atomic coordinates of a Lys49 PLA_2 isolated from the venom of *Ag. acutus* (PDB code 1mc2), stripped of solvent and ligand atoms, were used to generate the search model. The cross-rotation and translation functions were calculated over the resolution range 20.0–3.0 Å and the rotation angles which produced the peak with the highest correlation and the lowest R factor were applied to the search model for the translation search. The searches were performed for both enantiomorphic space groups ($P4_32_12$ and $P4_12_12$) and the correct solution was selected based on the crystallographic residual and the correlation coefficient. The model was subjected to isotropic restrained refinement using the program *REFMAC*5 (Murshudov *et al.*, 1997) and the structural model was improved based on $2F_o - F_c$ and $F_o - F_c$ electron-density maps, which were examined using the graphics program *TURBO-FRODO* (Roussel & Cambillau, 1991). During the refinement, residual density observed near Arg34 was attributed to a sulfate ion based on the tetrahedral shape of the density and the possible interactions. The refinement converged to an R factor of 22% and an R_{free} of 27% (Table 1).

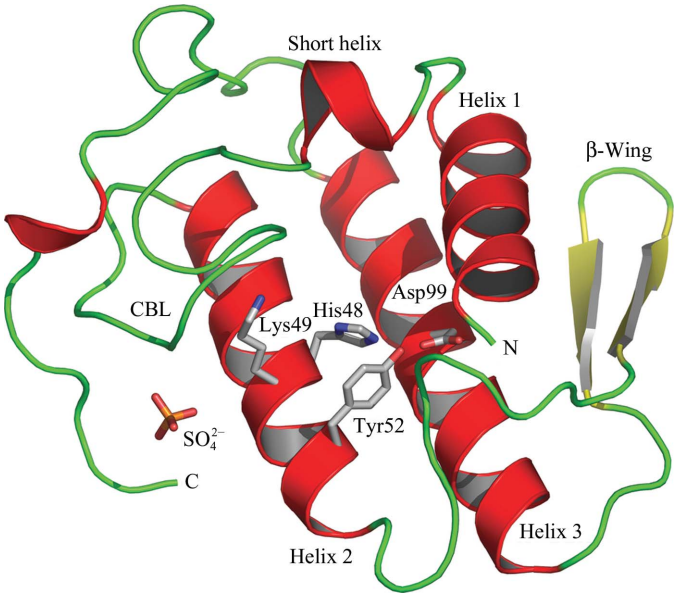

Figure 1
Cartoon representation of the *A. nummifer* myotoxin II (Anum-II) crystal structure. The residues which form the nominal active-site are presented in atom colours. CBL: putative calcium-binding loop.

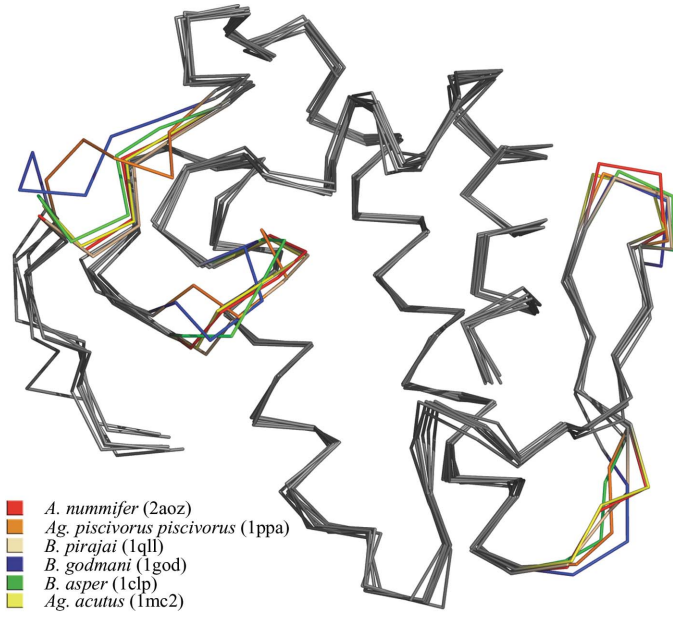

Figure 2
Superpositioning of Anum-II on the structures of *B. godmani* (PDB code 1god), *B. asper* (1clp, chain *A*), *Ag. piscivorus piscivorus* (1ppa), *B. pirajai* (1qll) and *Ag. acutus* (1mc2) Lys49 PLA_2s. The structural differences are highighted by utilizing different colours.

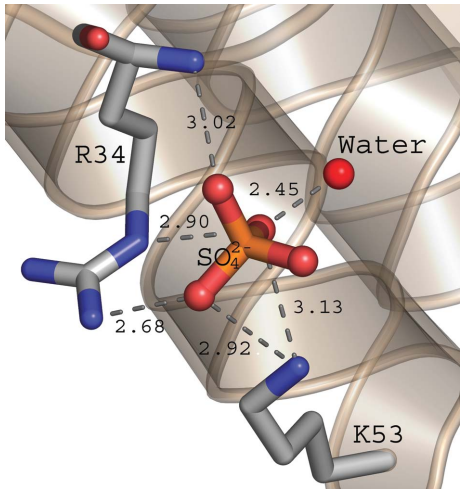

Figure 3
Interactions of the sulfate ion with Arg34 and Lys53 of Anum-II.

3. Results and discussion

3.1. Overall structure

The asymmetric unit of the Anum-II crystals consists of one protein molecule (121 amino-acid residues), one sulfate ion and 71 solvent water molecules. The quality of the model assessed by *PROCHECK* (Laskowski *et al.*, 1993) indicates that the stereochemical parameters lie within the expected range and the overall deviations from ideal stereochemistry are presented in Table 1. The Ramachandran diagram (Ramachandran *et al.*, 1963) indicates that 87% of the main-chain dihedral angles of all non-glycine and non-proline residues are located in the energetically most favoured regions, 12% are located in the additional permitted regions and only 1% lie in the generously permitted region. Based on the nomenclature and numbering scheme suggested by Renetseder *et al.* (1985), Anum-II can be classified as a class II PLA_2 enzyme and is stabilized by seven disulfide bridges (between residues 27 and 125, 29 and 45, 44 and 105, 50 and 133, 51 and 98, 61 and 91, and 84 and 96). The structures of PLA_2s have been extensively reviewed (Arni & Ward, 1996); briefly, the Anum-II structure can be considered to be formed of a short N-terminal α-helix (residues 2–12), a putative Ca^{2+}-binding loop (residues 25–35), a second α-helix (residues 40–55), a two-stranded antiparallel sheet referred to as the β-wing (residues 74–85) and a third α-helix (residues 90–107) that is antiparallel to the second; these two long helices are linked by two disulfide bridges to form a rigid platform. The positions of the amino-acid residues that form the catalytic apparatus (His48, Tyr52, Tyr73 and Asp99, including the catalytic water molecule) are conserved except for Asp49, which is substituted by Lys (Fig. 1). Superpositioning the Anum-II structure onto the structures of other Lys49 PLA_2s indicates that all structural features are conserved, with inherent flexibility observed in the C-terminus, putative calcium-binding loop, β-wing connecting loop and the tip of the β-wing (Fig. 2).

3.2. Anion-binding site

Clear density for a tetrahedral molecule was observed close to Arg34 in both the $2F_o - F_c$ and $F_o - F_c$ electron-density maps. Since the mother solution contains 0.2 *M* ammonium sulfate, this electron density was considered to represent a sulfate ion based on the geometry and possible hydrogen bonds. In this model, the O1 atom of the sulfate ion is anchored by hydrogen bonds to Arg34 N^{ε} (2.90 Å), Lys53 N^{ζ} (3.13 Å) and a solvent water molecule (2.45 Å). The O2 atom interacts with the main-chain NH group of Arg34 (3.02 Å) and the O4 atom with Lys53 N^{ζ} (3.38 Å) and Arg34 $N^{\eta 2}$ (2.68 Å) (Fig. 3). The crystal structure of *Ag. contortrix laticinctus* myotoxin also indicated the presence of a sulfate ion bound to Arg34 and Lys53 (Ambrosio *et al.*, 2005) and the sulfonyl group of the suramin molecule was shown to interact with Arg34 in *Bothrops asper* myotoxin II (Murakami *et al.*, 2005). This indicates that Arg34, which is strictly conserved in all Lys49 PLA_2s (Fig. 4), is likely to play a crucial role in the binding of negatively charged substrates or inhibitors.

3.3. Oligomeric state

The dimerization of Lys49 PLA_2s has been suggested to play an important role in their ability to damage membranes (de Oliveira *et al.*, 2001) and in the expression of cytolytic and myotoxic activities (Angulo *et al.*, 2005). Previous crystallographic results on the Lys49 PLA_2s *B. asper* myotoxin II (Arni *et al.*, 1995), *B. pirajai* piratoxin I (de Azevedo *et al.*, 1998) and *B. jararacussu* bothropstoxin I (Giotto *et al.*, 1998) suggested that the monomers present in the asymmetric unit are related by a twofold axis and that the dimer is stabilized by reciprocal interactions formed at the interface of the N-terminal and β-wing regions that encompass the conserved interfacial residues Glu12, Trp77 and Lys80 (Ward *et al.*, 1998; Ruller *et al.*, 2005). This quaternary arrangement stabilized by the Glu12–Lys80 salt bridge has been considered to represent the biologically relevant form (Ward *et al.*, 1998) and has been shown to be very stable.

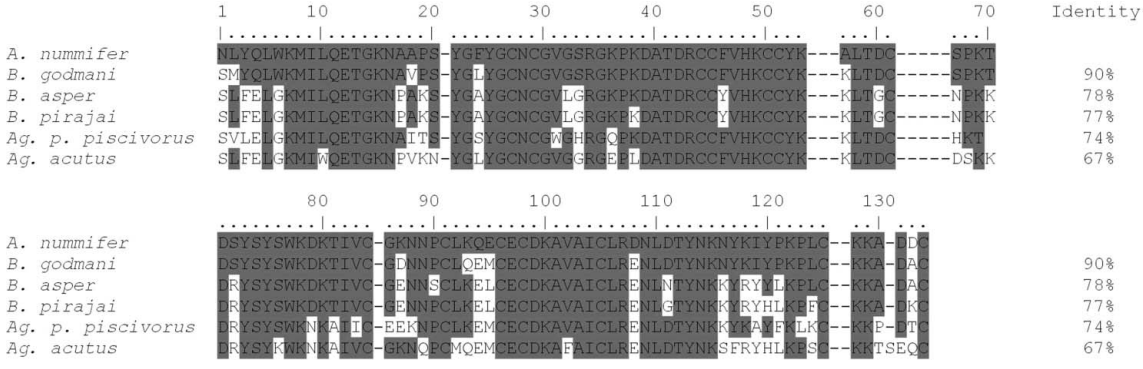

Figure 4
Sequence alignment of Anum-II with other Lys49 PLA_2s from *Cerrophidion (Bothrops) godmani* (PDB code 1god), *B. asper* (1clp), *Ag. piscivorus piscivorus* (1ppa), *B. pirajai* (1qll, chain *A*) and *Ag. acutus* (1mc2).

However, a Lys49 PLA_2 from *Deinagkistrodon acutus* (PDB code 1mg6; Huang *et al.*, unpublished work), myotoxin from *Ag. contortrix laticinctus* (PDB code 1s8g; Ambrosio *et al.*, 2005), myotoxin II from *Cerrophidion (Bothrops) godmani* (Arni *et al.*, 1999) and Anum-II (this work) exist as monomers in the crystalline state. Anum-II is present as a dimer in solution at physiological pH (Angulo *et al.*, 2000). Thus, the monomeric Anum II observed in the asymmetric unit may be an artifact of the crystallization process and the low pH of the solution (pH 5). In the case of bothropstoxin I (BthTX-I), the effect of pH on the monomer–dimer equilibrium was examined based on the fluorescent properties of the single Trp77 and it was shown that the monomeric form of the protein is predominant at acidic pH (de Oliveira *et al.*, 2001). Small-angle X-ray scattering studies currently in progress will be useful in clarifying the parameters that influence the equilibrium between monomers and dimers.

Financial support from FAPESP, CEPID/FAPESP, SMOLBNet (FAPESP), CNPq, CAPES/DAAD, FUNDUNESP and CONICIT (FV-058-02) is gratefully acknowledged. MTM is the recipient of a FAPESP fellowship.

References

Ambrosio, A. L., Nonato, M. C., de Araújo, H. S., Arni, R. K., Ward, R. J., Ownby, C. L., de Souza, D. H. & Garratt, R. C. (2005). *J. Biol. Chem.* **280**, 7326–7335.

Angulo, Y., Gutiérrez, J. M., Soares, A. M., Cho, W. & Lomonte, B. (2005). *Toxicon*, **46**, 291–296.

Angulo, Y., Olamendi-Portugal, T., Alape-Girón, A., Possani, L. D. & Lomonte, B. (2002). *Int. J. Biochem. Cell Biol.* **34**, 1268–1278.

Angulo, Y., Olamendi-Portugal, T., Possani, L. D. & Lomonte, B. (2000). *Int. J. Biochem. Cell Biol.* **32**, 63–71.

Arni, R. K., Fontes, M. R., Barberato, C., Gutiérrez, J. M., Díaz, C. & Ward, R. J. (1999). *Arch. Biochem. Biophys.* **366**, 177–182.

Arni, R. K. & Gutiérrez, J. M. (1993). *Toxicon*, **31**, 1061–1064.

Arni, R. K. & Ward, R. J. (1996). *Toxicon*, **34**, 827–841.

Arni, R. K., Ward, R. J., Gutiérrez, J. M. & Tulinsky, A. (1995). *Acta Cryst.* D**51**, 311–317.

Azevedo, W. F. de, Ward, R. J., Canduri, F., Soares, A., Giglio, J. R. & Arni, R. K. (1998). *Toxicon*, **36**, 1395–1406.

Azevedo, W. F. de, Ward, R. J., Gutiérrez, J. M. & Arni, R. K. (1999). *Toxicon*, **37**, 371–384.

Giotto, M. T. S., Garratt, R. C., Oliva, G., Mascarenhas, Y. P., de Azevedo, W. F., Giglio, J. R., Cintra, A. C. O., Arni, R. K. & Ward, R. J. (1998). *Proteins*, **30**, 442–454.

Gutiérrez, J. M. & Lomonte, B. (1995). *Toxicon*, **33**, 1405–1424.

Gutiérrez, J. M., Lomonte, B. & Cerdas, L. (1986). *Toxicon*, **24**, 885–894.

Laskowski, R. A., MacArthur, M. W., Moss, D. S. & Thornton, J. M. (1993). *J. Appl. Cryst.* **26**, 283–291.

Leslie, A. G. W. (1992). *Jnt CCP4/ESF–EACBM Newsl. Protein Crystallogr.* **26**.

Lomonte, B., Angulo, Y. & Calderón, L. (2003). *Toxicon*, **42**, 885–901.

Maraganore, J. M., Merutka, G., Cho, W., Welches, W., Kézdy, F. J. & Heinrikson, R. L. (1984). *J. Biol. Chem.* **259**, 13839–13843.

Mebs, D. & Ownby, C. L. (1990). *Pharmacol. Ther.* **48**, 223–236.

Murakami, M. T., Arruda, E. Z., Melo, P. A., Martinez, A. B., Calil-Elias, S., Tomaz, M. A., Lomonte, B., Gutierrez, J. M. & Arni, R. K. (2005). *J. Mol. Biol.* **350**, 416–426.

Murshudov, G. N., Vagin, A. A. & Dodson, E. J. (1997). *Acta Cryst.* D**53**, 240–255.

Nishioka, S. A. & Silveira, P. V. P. (1992). *Am. J. Trop. Med. Hyg.* **47**, 805–810.

Oliveira, A. H. C., Giglio, J. R., Andrião-Escarso, S. H., Ito, A. S. & Ward, R. J. (2001). *Biochemistry*, **40**, 6912–6920.

Ramachandran, G. N., Ramakrishnan, C. & Sasisekharan, V. (1963). *J. Mol. Biol.* **7**, 95–99.

Renetseder, R., Brunie, S., Dijkstra, B. W., Drenth, J. & Sigler, P. B. (1985). *J. Mol. Chem.* **260**, 11627–11636.

Roussel, A. & Cambillau, C. (1991). *Silicon Graphics Geometry Partners Directory*, p. 86. Mountain View, CA, USA: Silicon Graphics.

Ruller, R., Aragao, E. A., Chioato, L., Ferreira, T. L., de Oliveira, A. H., Sa, J. M. & Ward, R. J. (2005). *Biochimie*, **87**, 993–1003.

Scott, D. L., Achari, A., Vidal, J. C. & Sigler, P. B. (1992). *J. Biol. Chem.* **267**, 22645–22657.

Six, D. A. & Dennis, E. A. (2000). *Biochim. Biophys. Acta*, **1488**, 1–19.

Solórzano, A. (1989). *Rev. Biol. Trop.* **37**, 133–137.

Taylor, R., Flores, A., Flores, G. & Bolaños, R. (1974). *Rev. Biol. Trop.* **21**, 383–397.

Vagin, A. A. & Teplyakov, A. (1997). *J. Appl. Cryst.* **30**, 1022–1025.

Ward, R. J., de Azevedo, W. F. & Arni, R. K. (1998). *Toxicon*, **36**, 1623–1633.

Watanabe, L., Angulo, Y., Lomonte, B. & Arni, R. K. (2004). *Biochim. Biophys. Acta*, **1703**, 87–89.

Yamazaki, Y., Matsunaga, Y., Nakano, Y. & Morita, T. (2005). *J. Biol. Chem.* **280**, 29989–29992.